

Acoustic scattering by two fluid confocal prolate spheroids

E. F. Lavia

December 4, 2019

Abstract

The exact spheroidal-function series solution for the time-harmonic acoustic scattering of a plane wave by two fluid confocal prolate spheroids is developed and a numerical implementation is formulated and validated by independent methods. The two spheroids define three regions in which the acoustic fields are expanded in terms of spheroidal wave functions multiplied by unknown coefficients. These expansions are forced to satisfy the boundary conditions and by using the orthogonality properties of the involved functions an infinite matricial system for the coefficients is obtained. The resulting system is then solved through a truncation procedure. The implementation has no limitations regarding the sound speed and density of the three media involved or in the incidence frequency.

1 Introduction

The availability of exact solutions for certain acoustic scattering problems (involving simple geometries as spheres, cylinders, etc.) has been, besides its importance *per se*, of widespread utility since additionally they can be used as benchmark solutions to validate approximate but more general methods based on some kind of discretization (being the Finite Element Method –FEM– and the Boundary Element Method –BEM– maybe the most prominent examples). Furthermore exact solutions usually are also less prone to display limitations or problems in the high frequency regime.

In the case of acoustic scattering of harmonic plane waves by obstacles with those simple geometries, exact solutions found by using the separation-of-variables procedure exist when the obstacle surface can be identified with a coordinate surface that belongs to a coordinate system for which the Helmholtz equation is separable [1]. Restricting to second degree surfaces, the latter condition corresponds to eleven coordinate systems of which the spherical, cylindrical and prolate/oblate spheroidal surely are the most conspicuous [2] because they are the ones that best fit in relevant scattering situations.

Solutions for the scattering produced by the infinite circular fluid cylinder or the fluid sphere [3] are *classics* and usually conform the starting point of all introductory texts about penetrable acoustic scattering. The corresponding solutions for the acoustic elastic problem, when there are also shear waves in addition to compressional ones, appeared shortly afterwards [4, 5].

The same scheme used to obtain the solution for the scattering by a single obstacle (that is matching boundary conditions on a coordinate surface) can be used to build the solution for the scattering of two or more similar obstacles, each one inside the previous, because in that case the boundary conditions have to be verified in coordinate surfaces of the same type. In the spherical coordinate system, for example, that procedure leads naturally to the solution for the scattering by two concentric spheres (a setup which is called a *spherical*

shell). It is important to remark that the method provides a straightforward solution only if the spheres have the same origin, i.e. if they are concentric, because otherwise the boundary conditions do not correspond to evaluate the solution in a single coordinate surface.

Seminal studies on spherical and cylindrical shells appeared in the sixties [6–8]. Today these results are firmly set within *the canon* of highly verified acoustic scattering solutions. Subsequently many other works have considered them under different conditions [9–11].

The prolate and oblate spheroids, whose geometries make them susceptible to many practical acoustical applications, have been object of much interest [12–14]. Some of the special functions resulting from the separation of variables of the wave equation in these coordinate systems (the spheroidal wave functions [15–17]) display in their calculation difficulties greater than those corresponding to the spherical and cylindrical cases (spherical and cylindrical Bessel functions, respectively) which is why they usually require numerical precision beyond the current 64-bit hardware precision [18, 19]. The history of its calculation is very prolific, see [18–20] and references therein.

The exact analytical solution for the fluid spheroid appeared in 1964 [21]. Afterwards, different works dealing with numerical calculations were restricted to: certain particular cases of sound speed or density contrasts [22, 23], the low frequency regime [22, 24–28] or low eccentricity spheroids [29]. A numerical evaluation of the exact solution without any limitation, based on [21] and using a computational code [20] for spheroidal wave function calculation in arbitrary precision was presented in [30].

A configuration with two spheroids was addressed in [31], where scattering of a plane wave by a rigid prolate spheroid coated with a confocal sheat of penetrable (fluid) acoustic material was obtained. A system of multilayered confocal prolate spheroids, the innermost being considered rigid, was developed in [32] and then applied to the case of an spheroid coated with a single layer of fluid [33], providing thus a simplified model for a stone located in the human kidney. In all these works, the interior spheroid is always considered as an impenetrable one.

The elastic prolate spheroid was addressed in [34]. In that reference, the scattering from a prolate spheroidal shell was approximated by the response due to one in a resonant mode. Approximations for the scattering by spheroidal elastic shells in the resonance region and calculated with the T-matrix method are presented in [35].

This work presents a numerical evaluation of the *exact*, in terms of a series, solution for the acoustic scattering of two fluid prolate confocal spheroids (from now on this setup will be called an *spheroidal shell*) valid for any value of eccentricity and arbitrary fluid properties of the three involved physical mediums. The oblate case can be worked out following the same lines with only slight modifications, see for details [30]. In view of that, this work is devoted to the prolate spheroid. The numerical implementation was developed using a modified version of the computational codes by Adelman et al. [20].

This paper is structured as follows. In Section 2 the analytical solution for the acoustic scattering by the spheroidal shell is formulated. Section 3 provides the workings of the numerical implementation. In Section 4 several numerical verifications against certain limiting cases (spheroid tending to sphere) and with results provided by a BEM implementation are carried out. Computations of external and internal fields are also included. Conclusions of the work are summarized in Section 5.

2 Theory. Analytical solution

The time-harmonic acoustic scattering of a plane wave by an spheroidal shell can be solved, as said previously, by separating variables in prolate spheroidal coordinates (ξ, η, φ) [15]. These coordinates are defined by

$$\begin{cases} x = \frac{d}{2} [(\xi^2 - 1)(1 - \eta^2)]^{1/2} \cos \varphi \\ y = \frac{d}{2} [(\xi^2 - 1)(1 - \eta^2)]^{1/2} \sin \varphi \\ z = \frac{d}{2} \xi \eta, \end{cases} \quad (1)$$

where d is the interfocal distance of the ellipse of major semi-axis $a = (d/2) \xi$ and minor semi-axis $b = (d/2) (\xi^2 - 1)^{1/2}$. The values for the prolate spheroidal coordinates must verify $\xi \geq 1$, $-1 \leq \eta \leq 1$, and $0 \leq \varphi < 2\pi$. The parameter $d = 2(a^2 - b^2)^{1/2}$ defines a particular prolate spheroid system. The surface of any spheroid belonging to this system coincides with the coordinate surface given by $\xi = \xi_0$, with $\xi_0 = (1 - (b/a)^2)^{-1/2}$.

The scattering problem is depicted in Figure 1. The acoustic pressure of an incident plane wave with angular frequency ω , propagating in a surrounding medium of sound speed c_0 can be written as

$$p_i = p_0 \exp(ik_0 \hat{k} \cdot \mathbf{x}),$$

where $k_0 = \omega/c_0$ is the wave number, $\hat{k} = (\sin \theta_i \cos \varphi_i, \sin \theta_i \sin \varphi_i, \cos \theta_i)$ is the incidence direction (being θ_i, φ_i the spherical angles of incidence) and p_0 the amplitude. Without loss of generality, due to the symmetry of revolution around the z axis, it can be considered $\varphi_i = 0$ so that $\hat{k} = (\sin \theta_i, 0, \cos \theta_i)$ and the incidence is fully characterized by a single angle. Such incident wave on the prolate spheroidal shell is illustrated in Figure 1 and identified with the wave vector $\mathbf{k} = k_0 \hat{k}$.

The two spheroids constituting the shell have major and minor semiaxis a_1, b_1 and a_2, b_2 , respectively, and verify the condition

$$a_1^2 - b_1^2 = a_2^2 - b_2^2 = \left(\frac{d}{2}\right)^2, \quad (2)$$

which assures that the focal distance d is the same for both (i.e. the spheroids are confocal). Therefore, both spheroids are described by the same spheroidal system, related to cartesian coordinates by (1). The boundaries of the spheroids correspond to values ξ_0 and ξ_1 of the spheroidal coordinate ξ and define three regions characterized by different values of sound speed and density c_i, ρ_i ($i = 0, 1, 2$).

The procedure of separation of variables applied on the Helmholtz equation $(\nabla^2 + k^2)p = 0$ in the coordinates (ξ, η, φ) leads to a representation of the solution in terms of spheroidal angular functions $S_{mn}(h, \eta)$ and radial spheroidal functions of the first and second kinds, $R_{mn}^{(1)}(h, \xi)$ and $R_{mn}^{(2)}(h, \xi)$, respectively [15–17]. These functions also depend on the dimensionless parameter $h \equiv (d/2) k$, which characterizes the scattering in each medium through its corresponding wave number k .

Then, in each of the three regions a Helmholtz equation with a different wave number $k_i = \omega/c_i$, ($i = 0, 1, 2$) is valid so that the fields there are built of linear combinations of the $S_{mn}(h_i, \eta)$, $R_{mn}^{(1)}(h_i, \xi)$ and $R_{mn}^{(2)}(h_i, \xi)$ spheroidal wave functions with unknown coefficients. The continuity of the pressure and normal velocity at each boundary ξ_0, ξ_1 leads to a system

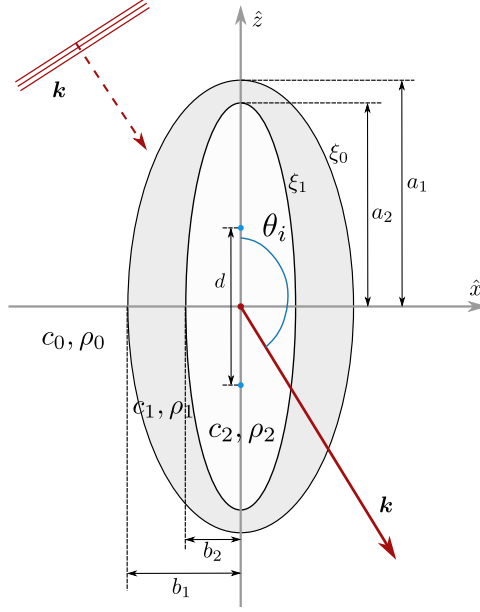


Figure 1: Coordinates for the scattering of a plane wave with incidence wave vector \mathbf{k} by two confocal prolate spheroids.

of matrix equations; since in this case there are four (two conditions times two boundaries) equations, then four matrix unknowns are expected.

In the following paragraphs the continuity equations will be transformed into a matrix system which will allow to solve the scattering problem for the spheroidal shell. The notation to be used closely follows the previous work [30].

In the surrounding medium (c_0, ρ_0) the pressure is the sum of the incident pressure p_i and the scattering pressure p_s ,

$$p = p_i + p_s. \quad (3)$$

The incident pressure p_i can be expanded on prolate spheroidal functions [16] and written as

$$p_i = 2p_0 \sum_{m,n \geq m} i^n \epsilon_m S_{mn}(h_0, \cos \theta_i) S_{mn}(h_0, \eta) R_{mn}^{(1)}(h_0, \xi) \cos(m\varphi),$$

where ϵ_m is the Neumann factor, defined as $\epsilon_m = 2$ if $m \neq 0$ and $\epsilon_m = 1$ if $m = 0$. The S_{mn} functions are assumed to be normalized, thus

$$\int_{-1}^1 [S_{mn}(h_i, \eta)]^2 d\eta = 1.$$

The scattered pressure field p_s can also be expressed as linear combination of spheroidal wave functions but using the radiating function $R^{(3)} \equiv R^{(1)} + iR^{(2)}$ (which diverges at $\xi = 1$) instead of the regular $R^{(1)}$; then

$$p_s = 2p_0 \sum_{m,n \geq m} i^n A_{mn} \epsilon_m S_{mn}(h_0, \cos \theta_i) S_{mn}(h_0, \eta) R_{mn}^{(3)}(h_0, \xi) \cos(m\varphi) \quad (4)$$

where A_{mn} is a matrix of expansion coefficients.

The pressure field inside the outer spheroid, which constitutes the (c_1, ρ_1) medium, can be written as a sum of a standing solution and a radiating solution, i.e.

$$p_1 = p_{1s} + p_{1r} \quad (5)$$

where

$$p_{1s} = 2p_0 \sum_{m,n \geq m} i^n B_{mn} \epsilon_m S_{mn}(h_0, \cos \theta_i) S_{mn}(h_1, \eta) R_{mn}^{(1)}(h_1, \xi) \cos(m\varphi), \quad (6)$$

$$p_{1r} = 2p_0 \sum_{m,n \geq m} i^n C_{mn} \epsilon_m S_{mn}(h_0, \cos \theta_i) S_{mn}(h_1, \eta) R_{mn}^{(3)}(h_1, \xi) \cos(m\varphi). \quad (7)$$

Finally, the pressure in the inner spheroid (which must be regular in $\xi = 1$) can be written as a standing wave,

$$p_2 = 2p_0 \sum_{m,n \geq m} i^n D_{mn} \epsilon_m S_{mn}(h_0, \cos \theta_i) S_{mn}(h_2, \eta) R_{mn}^{(1)}(h_2, \xi) \cos(m\varphi). \quad (8)$$

In the expressions (6), (7) and (8) the matrices B_{mn}, C_{mn}, D_{mn} are the corresponding coefficients to be determined.

In each interface, ξ_0 and ξ_1 , the boundary conditions of continuity of pressure and normal velocity must be applied. This leads to the following four equations:

$$(p_i + p_s)|_{\xi=\xi_0} = (p_{1s} + p_{1r})|_{\xi=\xi_0} \quad (9)$$

$$\frac{1}{\rho_0} \frac{\partial(p_i + p_s)}{\partial \xi} \Big|_{\xi=\xi_0} = \frac{1}{\rho_1} \frac{\partial(p_{1s} + p_{1r})}{\partial \xi} \Big|_{\xi=\xi_0} \quad (10)$$

$$(p_{1s} + p_{1r})|_{\xi=\xi_1} = p_2|_{\xi=\xi_1} \quad (11)$$

$$\frac{1}{\rho_1} \frac{\partial(p_{1s} + p_{1r})}{\partial \xi} \Big|_{\xi=\xi_1} = \frac{1}{\rho_2} \frac{\partial(p_2)}{\partial \xi} \Big|_{\xi=\xi_1} \quad (12)$$

In order to build the matrix system it is convenient, for the first two previous equations, to expand $S_{mn}(h_0, \eta)$ in terms of the set $\{S_{m\ell}(h_1, \eta) : \ell \geq m\}$ and, for the last two ones, $S_{mn}(h_1, \eta)$ in terms of the set $\{S_{m\ell}(h_2, \eta) : \ell \geq m\}$. Then,

$$S_{mn}(h_0, \eta) = \sum_{\ell=m}^{\infty} \alpha_{n\ell}^{(m)} S_{m\ell}(h_1, \eta) \quad \text{with} \quad \alpha_{n\ell}^{(m)} = \int_{-1}^1 S_{mn}(h_0, \eta) S_{m\ell}(h_1, \eta) d\eta \quad (13)$$

and

$$S_{mn}(h_1, \eta) = \sum_{\ell=m}^{\infty} \tilde{\alpha}_{n\ell}^{(m)} S_{m\ell}(h_2, \eta) \quad \text{with} \quad \tilde{\alpha}_{n\ell}^{(m)} = \int_{-1}^1 S_{mn}(h_1, \eta) S_{m\ell}(h_2, \eta) d\eta. \quad (14)$$

Substituting the expansion (13) in the LHS of Eqs. (9) and (10), and the expansion (14) in the LHS of Eqs. (11) and (12) and using the orthogonality properties of the families $\{S_{mn}(h_1, \eta) \cos(m\varphi) : m \geq 0, n \geq m\}$ and $\{S_{mn}(h_2, \eta) \cos(m\varphi) : m \geq 0, n \geq m\}$, four matrix equations involving the A_{mn}, B_{mn}, C_{mn} and D_{mn} coefficients are obtained.

It is convenient to define matrices

$$\begin{aligned} [Q^j(h, \xi)]_{\sigma n}^{(m)} &= i^n \alpha_{n\sigma}^{(m)} S_{mn}^{h_0} R_{mn}^{(j)}(h, \xi) & j = 3 \\ [Q^{j'}(h, \xi)]_{\sigma n}^{(m)} &= i^n \frac{\rho_1}{\rho_0} \alpha_{n\sigma}^{(m)} S_{mn}^{h_0} R_{mn}^{(j)'}(h, \xi) & j = 3 \\ [D^j(h, \xi)]_{\sigma n}^{(m)} &= i^n \delta_{n\sigma} S_{mn}^{h_0} R_{mn}^{(j)}(h, \xi) & j = 1, 3 \\ [D^{j'}(h, \xi)]_{\sigma n}^{(m)} &= i^n \delta_{n\sigma} S_{mn}^{h_0} R_{mn}^{(j)'}(h, \xi) & j = 1, 3 \end{aligned}$$

$$\begin{aligned} [\tilde{Q}^j(h, \xi)]_{\sigma n}^{(m)} &= i^n \tilde{\alpha}_{n\sigma}^{(m)} S_{mn}^{h_0} R_{mn}^{(j)}(h, \xi) \quad j = 1, 3 \\ [\tilde{Q}^{j'}(h, \xi)]_{\sigma n}^{(m)} &= i^n \frac{\rho_2}{\rho_1} \tilde{\alpha}_{n\sigma}^{(m)} S_{mn}^{h_0} R_{mn}^{(j)'}(h, \xi) \quad j = 1, 3, \end{aligned}$$

and vectors

$$\begin{aligned} F_\sigma^{(m)} &= \sum_{n=m}^{\infty} i^n S_{mn}^{h_0} \alpha_{n\sigma}^{(m)} R_{mn}^{(1)}(h, \xi) \\ G_\sigma^{(m)} &= \sum_{n=m}^{\infty} \frac{\rho_1}{\rho_0} i^n S_{mn}^{h_0} \alpha_{n\sigma}^{(m)} R_{mn}^{(1)'}(h, \xi) \end{aligned}$$

where the prime indicates the ξ -derivative (i.e. $' \equiv d/d\xi$), $\delta_{n\sigma}$ is the Kronecker delta and $S_{mn}^{h_0} \equiv S_{mn}(h_0, \cos \theta_i)$. The D^j and $D^{j'}$ matrices contains $\delta_{n\sigma}$, thus they are diagonal. This property is stressed by the “ D -letter” in his name. Care must be taken in avoiding to mix those matrices with the unknown coefficients D_{mn} .

Then, it can be shown that for each fixed $m = 0, 1, 2, \dots$ the four matrix equations set leads to a infinite matrix system

$$\begin{pmatrix} Q^3(h_0, \xi_0)^{(m)} & -D^1(h_1, \xi_0)^{(m)} & -D^3(h_1, \xi_0)^{(m)} & 0 \\ Q^{3'}(h_0, \xi_0)^{(m)} & -D^{1'}(h_1, \xi_0)^{(m)} & -D^{3'}(h_1, \xi_0)^{(m)} & 0 \\ 0 & \tilde{Q}^1(h_1, \xi_1)^{(m)} & \tilde{Q}^3(h_1, \xi_1)^{(m)} & -D^1(h_2, \xi_1)^{(m)} \\ 0 & \tilde{Q}^{1'}(h_1, \xi_1)^{(m)} & \tilde{Q}^{3'}(h_1, \xi_1)^{(m)} & -D^{1'}(h_2, \xi_1)^{(m)} \end{pmatrix} \begin{pmatrix} A^{(m)} \\ B^{(m)} \\ C^{(m)} \\ D^{(m)} \end{pmatrix} = \begin{pmatrix} -F^{(m)} \\ -G^{(m)} \\ 0 \\ 0 \end{pmatrix}. \quad (15)$$

The index m was indicated as a superscript to emphasize the fact that for each fixed m a matrix system of the type (15) has to be solved. Each of these solutions provides a vector including the four coefficients $A^{(m)}, B^{(m)}, C^{(m)}, D^{(m)}$, which contain all the corresponding n -values ($n = m, m+1, \dots$) for that index m . Once the coefficients for all m have been obtained, the fields p , p_1 and p_2 in each region can be evaluated.

In the far-field limit it can be shown [21] that, with respect to spherical coordinates (r, θ, φ) of the observation point, the scattering pressure p_s is given by

$$p_s(r, \theta, \varphi) \approx p_0 \frac{e^{ik_0 r}}{r} f_\infty(\theta, \varphi),$$

where $f_\infty(\theta, \varphi)$ is the so-called far-field scattering amplitude function which is widespreadly used in different acoustic scattering applications. In the particular case of an spheroidal shell, it results

$$f_\infty(\theta, \varphi) = \frac{2}{ik_0} \sum_{m, n \geq m} A_{mn} \epsilon_m S_{mn}(h_0, \cos \theta_i) S_{mn}(h_0, \cos \theta) \cos(m\varphi). \quad (16)$$

3 Numerical implementation

To numerically calculate the set of coefficients $\{A, B, C, D\}$ a truncation procedure must be carried out. The first step is to select a maximum value M for the index m . Then, $M+1$ matricial systems (15) labeled with a distinct value m results. The system $m=0$ has $M+1$ unknowns $A_n^{(0)}$ ($n = 0, 1, \dots, M$) and, equivalently, the same number of the other coefficients. By considering that the subsequent matricial systems $m=1, m=2, \dots, m=M$ have the same size, this leads to $4(M+1)^2$ unknowns $A_n^{(m)}, B_n^{(m)}, C_n^{(m)}, D_n^{(m)}$ where the label n takes the values $n = m, m+1, \dots, m+M$.

In summary, each matricial system will have a size $4(M+1) \times 4(M+1)$ and its solution will provide the corresponding m -set of $4(M+1)$ coefficients $A_n^{(m)}$, $B_n^{(m)}$, $C_n^{(m)}$ and $D_n^{(m)}$ with $n \in [m, m+M]$.

For example, in an hypothetical case of $M = 5$ there will be six systems (15) of size 36×36 , each one identified by $m = 0, 1, \dots, 5$. The solution of any m -system provides a vector

$$(A_0^m, A_1^m, \dots, A_5^m, B_0^m, B_1^m, \dots, B_5^m, C_0^m, C_1^m, \dots, C_5^m, D_0^m, D_1^m, \dots, D_5^m).$$

Finally, the 6×6 matrix of coefficients A_n^m results in

$$A = \begin{pmatrix} A_0^0 & A_1^1 & \dots & A_5^5 \\ A_0^1 & A_1^2 & \dots & A_6^5 \\ \dots & \dots & \dots & \dots \\ A_0^5 & A_1^6 & \dots & A_{10}^5 \end{pmatrix},$$

where the m -th column comes from the numerical solution of the m -system. The other coefficient matrices B, C, D can be arranged in a similar fashion.

The key idea in this truncation procedure is that for some truncation number M the obtained values for all no negligible coefficients should not change; then, a subsequent increase in the size of the system (i.e. a new truncation number greater than M) must not alter the solution.

Convergence for a certain coefficient in the system is achieved when an increment in the truncation number M does not appreciably change the coefficient value. As stated above, convergence for a particular acoustic problem will be achieved when the successive coefficients that appear as a consequence of considering bigger M values not lead to a appreciable change in the numerical solution. Indicators of the occurrence of that situation usually will be coefficients tending to zero. However, to avoid false identifications, care must be taken in selecting the appropriate M and avoid falling in stagnation zones where the coefficients are small for certain m, n but rise for m, n greater.

In the $M = 5$ example provided above, the subsequent approximation $M = 6$ involves thirteen new coefficients $A_6^0, A_7^1, \dots, A_{12}^6, A_6^6, A_7^6, \dots, A_{11}^6$. Even if all of them were negligible, it could happen that within the subsequent coefficients appearing for $M = 7$, for example, some were not negligible and thus necessary to obtain a convergent solution. In any case, a calculation for excess in the coefficients is mandatory as well as a good habit.

Coefficients of negligible value are not, however, the sole indicator of convergence because it could happen that these coefficients were multiplied in the expansion by spheroidal functions that may take very high values for particular choices of their arguments. Again, to watch over the emergence of this type of pathological behavior is another good habit.

4 Verifications

In the limiting cases of b_i tending to a_i ($i = 1, 2$) the two confocal spheroids tends to conform a spherical shell. Since the scattering by a spherical shell has exact solution, expressed in terms of spherical Bessel functions, it can be compared with the scattering resulting from an spheroidal shell at this geometrical limit.

In the spheroidal system $a_i = b_i$ is a prohibited value because in that case $d = 0$ and the system (1) becomes singular but nothing precludes to use b_i values near its corresponding a_i values and consequently considering an approximated spherical shell. For the validity of the confocal spheroidal shell model the values a, b must verify the relation (2). Fixing arbitrarily $a_1 = 0.5$, $a_2 = 0.25$ and $b_1 = 0.4999$ according to (2) the remaining b_2 has the

value $b_2 = 0.24979993995195438$. Using these values the farfield angular pattern $|f_\infty|$ for the spheroidal shell is compared against the exact spherical solution for the frequencies $f = 5$ kHz and $f = 10$ kHz and c_i, ρ_i parameters according to Table 1 (typical values in underwater acoustics applications).

Medium	c (m s ⁻¹)	ρ (kg m ⁻³)
0 (water)	1477.4	1026.8
1	$1.04 c_0$	$1.04 \rho_0$
2	$0.23 c_0$	$0.00129 \rho_0$

Table 1: Material properties (sound speed c and density ρ) for the spherical and spheroidal shell acoustic scattering problem.

The results are shown in Figure 2. The top panel shows the 5 kHz frequency case whereas the bottom one shows the corresponding to 10 kHz. The spherical shell (solid lines) and the spheroidal shell (dashed lines) are in good agreement. For the spheroidal shell model, the truncation parameter M used in the numerical solution is explicitly indicated into the legend of the graphic window. Note that a M value entails $(M + 1) \times (M + 1)$ coefficients (cf. Section 3).

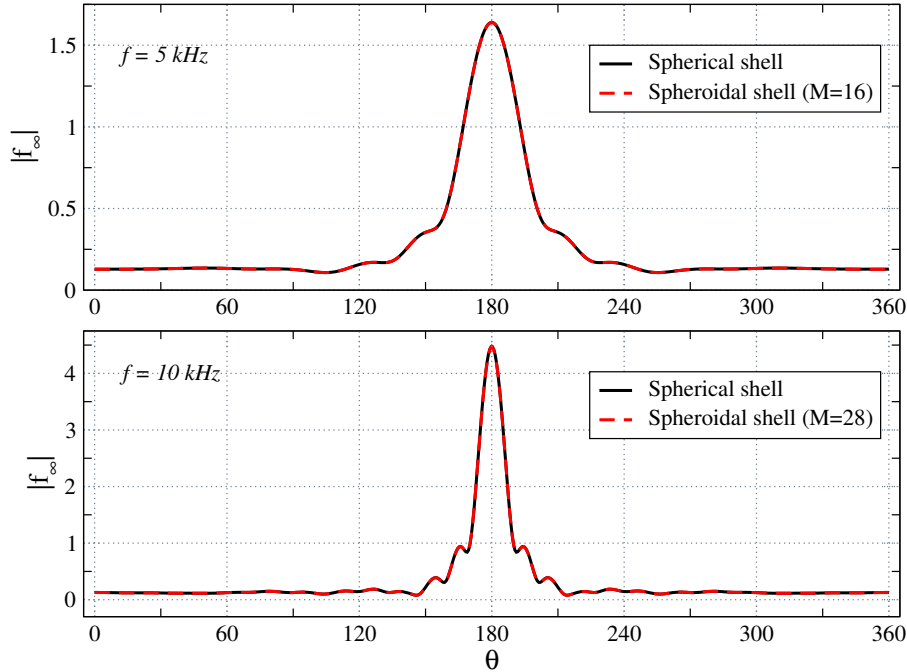


Figure 2: Farfield angular pattern $|f_\infty|$ in terms of the observation angle θ for a spherical shell (solid lines) and a spheroidal shell (dashed lines) in the geometrical limit when the spheroids tend to spheres. The incidence angle was $\theta_i = 180^\circ$.

With an increase in frequency generally more coefficients are necessary to achieve a converged solution; so for the 5 kHz case $M = 16$ were sufficient but for $f = 10$ kHz $M = 28$ were necessary. Notice that these M values corresponds to a converging solution for the external field p_s of Eq. (4). It is not guaranteed that the same external M -value will be sufficient for a converging solution for the internal fields p_1 and p_2 . In general, the

$h \equiv (d/2)k$ parameter characterize the scattering in a such a way that a higher value of h implies a more oscillatory behavior and consequently more coefficients in the solution are necessary to achieve convergence.

In order to verify the behavior of the model in a true spheroidal geometry, a Boundary Element Method (BEM) implementation for the acoustic problem of two confocal spheroids was implemented. The BEM method involves surface integration over the scatterer's boundaries. The usual approach is to consider a discretized version of each scattering surface, i.e. a *mesh*, composed by simpler elements as triangular or quadrilateral facets, which can be planar or curved. Then, the boundary integral is converted into a sum of integrations over the mesh elements.

Because the BEM method is an approximation it is expected that its solutions will be only a good approximation to an exact solution. Nevertheless, if the number of elements in the mesh is greater enough, the method allows for achieving a good agreement with an exact solution.

A usual prescription to ensure the preceding condition is to demand that the length ℓ of each segment that constitutes the mesh verifies a relation

$$\ell \leq \lambda/\beta, \quad (17)$$

where β is 5 or 6 [36]. Qualitatively this ensures that the field over the surface is *well* represented.

To test the model in a *true* confocal spheroidal shell configuration an outer spheroid of $a_1 = 0.5$ m and $b_1 = 0.25$ m and an inner one of $a_2 = 0.46$ m and $b_1 = 0.1552417$ m were considered. The material properties of the three media involved are the same ones tabulated in Table 1.

Two meshes representing the external and internal spheroids were built. The external mesh has $N_E = 21324$ triangular elements whereas the interior one has $N_I = 12380$. The maximum segment length in each case was 0.019768 m and 0.0174027 m, respectively, which implies that the maximum wavelengths λ that verify (17) (in the more strict condition $\beta = 6$) are 0.118608 m and 0.1044162 m. With these values a maximum frequency f_{\max} can be calculated for the scattering problem in question, in such a way that it is guaranteed that for frequencies less or equal to f_{\max} all the fields are well represented.

Since there are three sound speeds involved in the problem it follows that the safest situation corresponds to taking the slowest sound speed and the longest wavelength; that is, to consider the lowest of the maximum frequencies. Taking into account the material properties from Table 1 and the aforementioned meshes, a $f_{\max} = 2865$ Hz value is obtained. This does not mean, of course, that scattering evaluation for a frequency greater than the determined f_{\max} will fail catastrophically past over that threshold but only that gradual departures are expected as the frequency increases beyond that barrier.

In the Figure 3 two meshes for the confocal spheroidal setup are displayed. In this case, only for clarity purposes, the meshes have a reduced number of elements (2248 and 1484 for the external and internal mesh, respectively) so that individual triangles are clearly appreciated. The external spheroid mesh has also part of its surface removed to allow visualizing the internal one.

Figure 4 shows the resulting angular pattern for the absolute value of the f_{∞} for the frequency $f = 2$ kHz and incidence angle $\theta_i = \pi/4$, evaluated with the BEM formulation (dashed lines), using the meshes $\{N_E, N_I\}$, and the spheroidal shell model with $M = 20$ (solid lines). Both curves match.

For the same incidence but $f = 30$ kHz, a frequency value for which the present meshes are clearly insufficient for a *well represented* scattering, the $|f_{\infty}|$ is shown in Figure

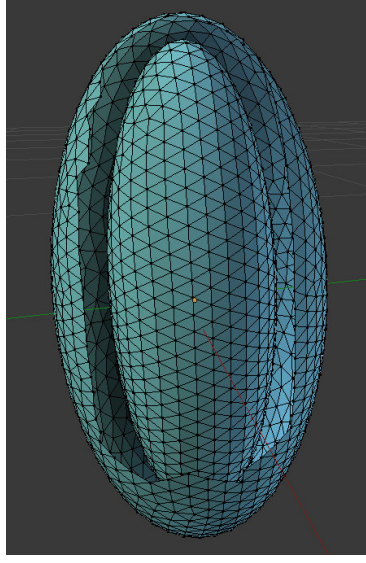


Figure 3: Illustrative mesh for the spheroidal shell. The external and internal spheroid meshes have $N = 2248$ and $N = 1484$ triangles, respectively. The exterior spheroid has some triangles removed so that the presence of the internal one is evident.

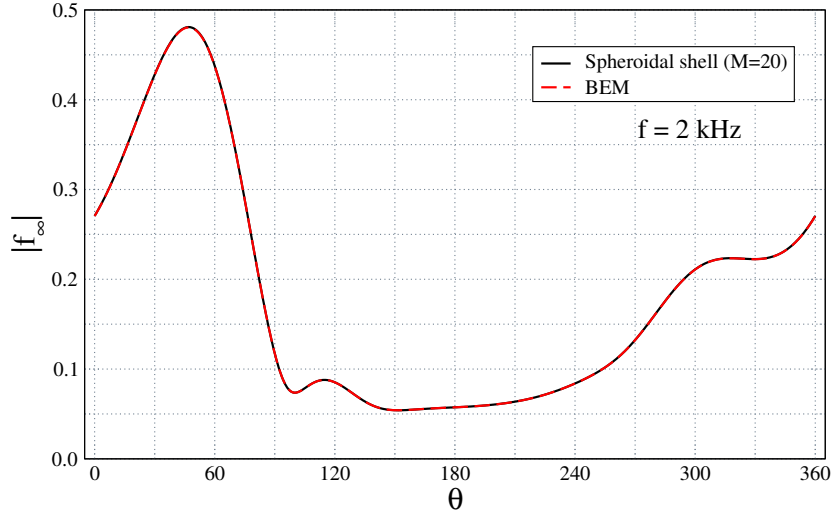


Figure 4: Farfield angular pattern $|f_\infty|$ in terms of the observation angle θ for the spheroidal shell at frequency $f = 2$ kHz. The incidence angle was $\theta_i = \pi/4$.

5. At this frequency, the BEM solution exhibits clear departures from the spheroidal shell solution. In this case, the spheroidal shell model has required $M = 220$ to ensure convergence. The parameters h for this problem are $h_0 = 55.24$, $h_1 = 53.119$ and $h_2 = 240.19$, so it is a high frequency case.

Finally, to make use of all the solution coefficients A, B, C, D , a nearfield calculation is carried out. Since this solution will not be compared with a benchmark, material media properties and frequency were selected to produce an aesthetically more pleasant plot. The two confocal spheroids retained the previously used maximum and minimum radius but the frequency was set to $f = 7.5$ kHz and the material properties were according to Table 2. The amplitude and incidence angle of the incident wave were $p_0 = 1$ and $\theta_i = \pi/4$, respectively.

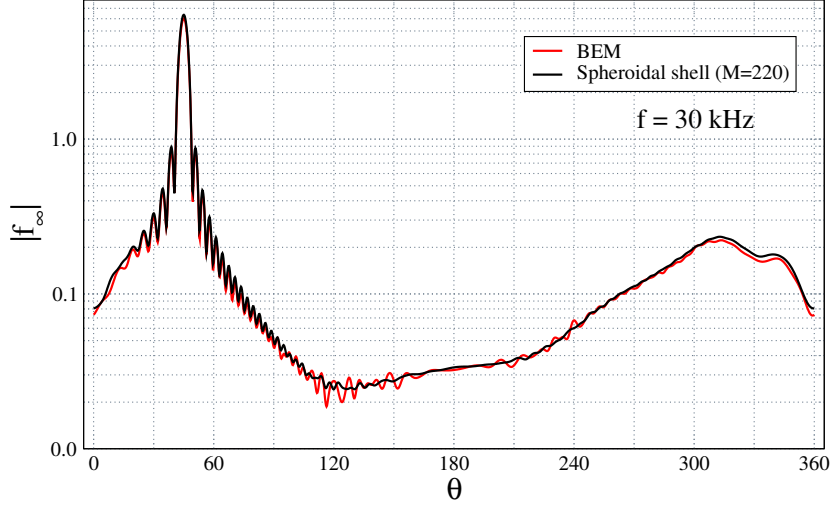


Figure 5: Absolute value of the farfield angular pattern $|f_\infty|$ in terms of the observation angle θ for two confocal spheroids at frequency $f = 30$ kHz. The incidence angle was $\theta_i = \pi/4$.

Medium	c (m s $^{-1}$)	ρ (kg m $^{-3}$)
0 (water)	1477.4	1026.8
1	$3 c_0$	$1.25 \rho_0$
2	$1.5 c_0$	$2.25 \rho_0$

Table 2: Material properties (sound speed c and density ρ) for nearfield evaluation.

In Figure 6 (left panel) the real part of the total field is shown in the interior of each spheroid and also in its surroundings, evaluated over the plane $y = 0$. The right panel of the figure exhibits the real part of the scattered field which exists only in the exterior to the external spheroid. The incidence direction is indicated by an arrow in both panels. The solution of the field in all regions required $M = 40$ and the parameters h were $h_0 = 5.98$, $h_1 = 1.99$ and $h_2 = 3.98$ so it is, indeed, an intermediate frequency scattering problem.

The total field displays no continuity problems or artifacts when crossing each one of the spheroid's boundaries, indicated on the figure by ellipses. This constitutes an indirect verification of the solution since the field in points located near each boundary but at opposite sides have been calculated through a different set of coefficients but they show, however, due to continuity, no abrupt changes in the field values. A shadow zone in the opposite side of the incidence is noticeable as well as an intense field value zone in the innermost spheroid.

The scattered field displayed in the right panel seems to correspond to a spherical source located in some point at the bottom of the shell, modified by the presence of the incident field in the previously mentioned shadow zone. Of course, this is expected because a total field near zero corresponds to $p_s \sim -p_i$, according to Eq. (3).

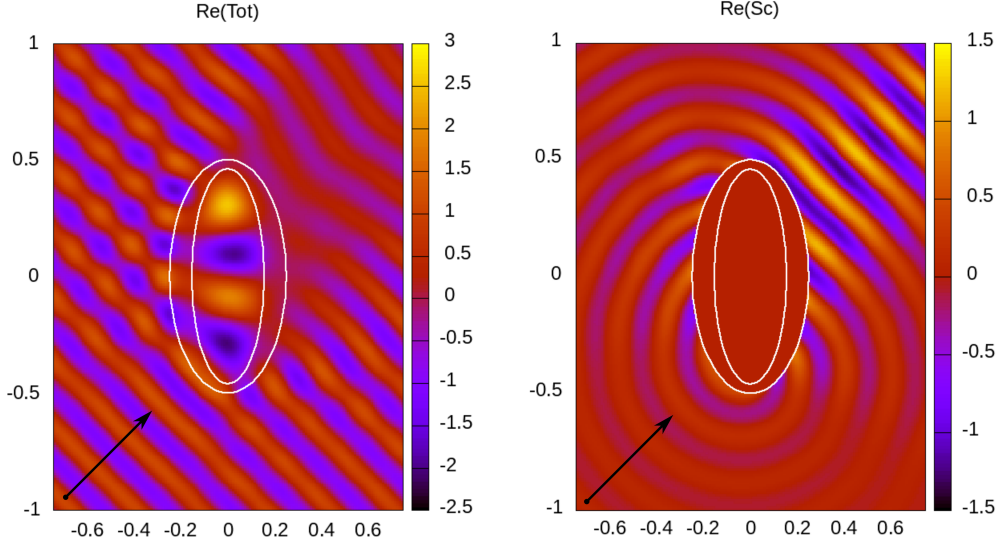


Figure 6: Real parts of the total (left) and the scattered (right) pressure field evaluated over the plane $y = 0$ in the nearfield region of the spheroidal shell. The incident field considered has amplitude $p_0 = 1$ and incidence angle $\theta_i = \pi/4$ (the incidence direction is indicated by an arrow).

5 Conclusions

A model to calculate the external and internal fields in the case of two confocal spheroids (an spheroidal shell) was presented. The required spheroidal wave function evaluation is carried out by using a previously published code, modified and optimized by the author to take advantage of parallel execution and also to strengthen high frequency calculations.

Numerical verifications against spherical shell and BEM solutions under certain circumstances allow to infer that the model adequately solves the scattering problem in a wide frequency interval. It must be noted that for a very high frequency regime the spheroidal wave function evaluations are computationally expensive but in this situation it is very likely that their asymptotic expressions can be used to alleviate that burden. However, it should be ensured that differences with exact evaluations under this regime would be negligible.

The procedure used for the numerical calculation of the coefficients follows closely the classical one for spherical coordinates but instead must be solved by truncation. The scattering problem for a multilayered spheroidal shell with three or more surfaces can be worked out following the same lines.

If care is taken into account for determining the convergence conditions while ensuring the correct evaluation of the spherical wave functions, the presented model for scattering from confocal prolate spheroids can be added to the toolkit of exact solutions of the computational physicist devoted to acoustics.

Acknowledgments

The author wish to thank to Dr. Juan D. Gonzalez and M. Sc. Silvia Blanc for their valuable comments about mathematical and physical aspects of the problem as well as his scrupulous reading of the manuscript.

References

- [1] P. M. Morse, *Vibration and sound*. McGraw-Hill New York, 1948.
- [2] P. Moon and D. E. Spencer, *Field theory handbook, including coordinate systems, differential equations and their solutions*. Springer, 1971.
- [3] V. C. Anderson, “Sound scattering from a fluid sphere,” *The Journal of the Acoustical Society of America*, vol. 22, no. 4, pp. 426–431, 1950.
- [4] J. J. Faran Jr, “Sound scattering by solid cylinders and spheres,” *The Journal of the acoustical society of America*, vol. 23, no. 4, pp. 405–418, 1951.
- [5] R. Hickling, “Analysis of echoes from a solid elastic sphere in water,” *the Journal of the Acoustical Society of America*, vol. 34, no. 10, pp. 1582–1592, 1962.
- [6] R. R. Goodman and R. Stern, “Reflection and transmission of sound by elastic spherical shells,” *The Journal of the Acoustical Society of America*, vol. 34, no. 3, pp. 338–344, 1962.
- [7] R. Hickling, “Analysis of echoes from a hollow metallic sphere in water,” *The Journal of the Acoustical Society of America*, vol. 36, no. 6, pp. 1124–1137, 1964.
- [8] R. Doolittle and H. Überall, “Sound scattering by elastic cylindrical shells,” *The Journal of the Acoustical Society of America*, vol. 39, no. 2, pp. 272–275, 1966.
- [9] J. McNew, R. Lavarello, and W. D. O’Brien Jr, “Sound scattering from two concentric fluid spheres,” *The Journal of the Acoustical Society of America*, vol. 125, no. 1, pp. 1–4, 2009.
- [10] G. C. Everstine, G. C. Gaunaurd, and H. Huang, “Acoustic scattering by two submerged spherical shells: Numerical validation,” *Journal of Computational Acoustics*, vol. 6, no. 04, pp. 421–434, 1998.
- [11] S. A. Cummer, B.-I. Popa, D. Schurig, D. R. Smith, J. Pendry, M. Rahm, and A. Starr, “Scattering theory derivation of a 3d acoustic cloaking shell,” *Physical review letters*, vol. 100, no. 2, p. 024301, 2008.
- [12] R. Spence and S. Granger, “The scattering of sound from a prolate spheroid,” *The Journal of the Acoustical Society of America*, vol. 23, no. 6, pp. 701–706, 1951.
- [13] V. Varadan, V. Varadan, L. R. Dragonette, and L. Flax, “Computation of rigid body scattering by prolate spheroids using the t-matrix approach,” *The Journal of the Acoustical Society of America*, vol. 71, no. 1, pp. 22–25, 1982.
- [14] J. A. Roumeliotis, A. D. Kotsis, and G. Kolezas, “Acoustic scattering by an impenetrable spheroid,” *Acoustical Physics*, vol. 53, no. 4, pp. 436–447, 2007.
- [15] P. M. Morse and H. Feshbach, *Methods of Theoretical Physics*. McGraw Hill Book Company, New York, 1953.
- [16] C. Flammer, *Spheroidal Wave Functions*. Stanford University press, Stanford, California, 1957.
- [17] E. Skudrzyk, *The foundations of acoustics: basic mathematics and basic acoustics*. Springer-Verlag, Wien, 1971.

- [18] A. L. Van Buren and J. E. Boisvert, “Improved calculation of prolate spheroidal radial functions of the second kind and their first derivatives,” *Quarterly of Applied Mathematics*, vol. 62, no. 3, pp. 493–507, 2004.
- [19] P. E. Falloon, P. Abbott, and J. Wang, “Theory and computation of spheroidal wave-functions,” *Journal of Physics A: Mathematical and General*, vol. 36, no. 20, p. 5477, 2003.
- [20] R. Adelman, N. A. Gumerov, and R. Duraiswami, “Software for computing the spheroidal wave functions using arbitrary precision arithmetic,” *arXiv:1408.0074v1 [cs.MS]*, 2014.
- [21] C. Yeh, “The diffraction of sound waves by penetrable disks,” *Annalen der Physik*, vol. 468, no. 1-2, pp. 53–61, 1964.
- [22] C. Yeh, “Scattering of acoustic waves by a penetrable prolate spheroid. i. liquid prolate spheroid,” *The Journal of the Acoustical Society of America*, vol. 42, no. 2, pp. 518–521, 1967.
- [23] I. Prario, J. Gonzalez, A. Madirolas, and S. Blanc, “A prolate spheroidal approach for fish target strength estimation: modeling and measurements,” *Acta Acustica united with Acustica*, vol. 101, no. 5, pp. 928–940, 2015.
- [24] J. E. Burke, “Scattering by penetrable spheroids,” *The Journal of the Acoustical Society of America*, vol. 43, no. 4, pp. 871–875, 1968.
- [25] N. G. Einspruch and C. A. Barlow Jr, “Scattering of a compressional wave by a prolate spheroid,” *Quarterly of Applied Mathematics*, vol. 19, no. 3, pp. 253–258, 1961.
- [26] M. Furusawa, “Prolate spheroidal models for predicting general trends of fish target strength,” *Journal of the Acoustical Society of Japan (E)*, vol. 9, no. 1, pp. 13–24, 1988.
- [27] Z. Ye, “Low-frequency acoustic scattering by gas-filled prolate spheroids in liquids,” *The Journal of the Acoustical Society of America*, vol. 101, no. 4, pp. 1945–1952, 1997.
- [28] Y. Tang, Y. Nishimori, and M. Furusawa, “The average three-dimensional target strength of fish by spheroid model for sonar surveys,” *ICES Journal of Marine Science*, vol. 66, no. 6, pp. 1176–1183, 2009.
- [29] A. Kotsis and J. Roumeliotis, “Acoustic scattering by a penetrable spheroid,” *Acoustical Physics*, vol. 54, no. 2, pp. 153–167, 2008.
- [30] J. D. González, E. F. Lavía, and S. Blanc, “A computational method to calculate the exact solution for acoustic scattering by fluid spheroids,” *Acta Acustica united with Acustica*, vol. 102, no. 6, pp. 1061–1071, 2016.
- [31] C. Yeh, “Scattering by liquid-coated prolate spheroids,” *The Journal of the Acoustical Society of America*, vol. 46, no. 3B, pp. 797–801, 1969.
- [32] A. Charalambopoulos, G. Dassios, D. Fotiadis, and C. Massalas, “Scattering of a point generated field by a multilayered spheroid,” *Acta mechanica*, vol. 150, no. 1-2, pp. 107–119, 2001.

- [33] A. Charalambopoulos, D. Fotiadis, and C. Massalas, “Scattering of a point generated field by kidney stones,” *Acta mechanica*, vol. 153, no. 1-2, pp. 63–77, 2002.
- [34] A. Silbiger, “Scattering of sound by an elastic prolate spheroid,” *The Journal of the Acoustical Society of America*, vol. 35, no. 4, pp. 564–570, 1963.
- [35] G. C. Gaunaurd and M. F. Werby, “Acoustic Resonance Scattering by Submerged Elastic Shells,” *Applied Mechanics Reviews*, vol. 43, pp. 171–208, 08 1990.
- [36] S. Marburg, “Six boundary elements per wavelength: Is that enough?,” *Journal of Computational Acoustics*, vol. 10, no. 01, pp. 25–51, 2002.